POLITECNICO DI TORINO
Repository ISTITUZIONALE

Integration of thermochemical energy storage in concentrated solar power. Part 2: Comprehensive optimization of supercritical CO2 power block

Original
Integration of thermochemical energy storage in concentrated solar power. Part 2: Comprehensive optimization of supercritical CO2 power block / Tesio, U.; Guelpa, E.; Verda, V.. - In: ENERGY CONVERSION AND MANAGEMENT. X. - ISSN 2590-1745. - 6:(2020), p. 100038. [10.1016/j.ecmx.2020.100038]

Availability:
This version is available at: 11583/2842814 since: 2020-08-20T17:48:16Z

Publisher:
Elsevier Ltd

Published
DOI:10.1016/j.ecmx.2020.100038

Terms of use:

This article is made available under terms and conditions as specified in the corresponding bibliographic description in the repository

Publisher copyright
Elsevier postprint/Author's Accepted Manuscript

© 2020. This manuscript version is made available under the CC-BY-NC-ND 4.0 license http://creativecommons.org/licenses/by-nc-nd/4.0/.The final authenticated version is available online at: http://dx.doi.org/10.1016/j.ecmx.2020.100038

(Article begins on next page)

14 November 2024

Energy Conversion and Management: X 6 (2020) 100038

Contents lists available at ScienceDirect

Energy Conversion and Management: X

journal homepage: www.journals.elsevier.com/energy-conversion-and-management-x

Integration of thermochemical energy storage in concentrated solar power. Part 2: Comprehensive optimization of supercritical CO_2 power block

U. Tesio*, E. Guelpa, V. Verda

Energy Department, Politecnico di Torino, Turin, Italy

ARTICLE INFO

Keywords:
Pinch analysis
HEATSEP
Superstructure
Multi-objective optimization
100% renewable
Sustainability

ABSTRACT

Among the various options of Thermo-Chemical Energy Storage, Calcium-Looping represents a promising alternative for Concentrated Solar Power plants, thanks to high operating temperatures, high energy density and absence of thermal losses. Finding the most suitable power cycle for this system is a task that has still to be solved and is not trivial because it consists in a complex process synthesis problem. From a preliminary analysis (Part 1), supercritical CO_2 cycles results to be the most promising option. In the present work, the integration of this power block (pilot plant size, 2 MW_e) is deeply investigated through a comprehensive analysis. Numerous thermal cycle layouts are considered and two options for the power block thermal feeding are assumed. The HEATSEP methodology (comprising genetic algorithm, pinch analysis and bisection) is adopted to optimize both components operating conditions and heat transfer processes in the discharging phase. The plant section devoted to the charging process is optimized and dimensioned taking into account the transient operation. Thanks to the complex problem structure developed, the algorithm is free to find the most suitable configuration between a huge set of feasible combinations. Both energy and economic optimizations are performed for the complete plant and, being in contrast between them, a multi-objective optimization is executed. The independent variables influence on the resulting configuration is assessed and intermediate layouts obtained from the Pareto curve are commented. Carbonator inlet temperature of reactants are observed to increase with plant efficiency. The maximum efficiency (21%) is obtained with the most complex power block (recompression, intercooling and reheating) exchanging heat directly on the carbonator wall. Less performing discharging processes are cheaper but determine higher costs of charging sections; the resulting effect is positive and the integration of simpler power blocks results economically convenient. A power cycle with single intercooling and thermal feeding performed on the carbonator outflows is the result of economic optimization (efficiency equal to 16.3%). The algorithm gives precedence to power block thermal feeding and then to reactants preheating. Novel plant layouts are designed for these configurations and data useful for further investigations are provided in the last part of this work.

1. Introduction

The cost reduction expected for the Concentrated Solar Power (CSP) upscaling [1] arouse much interest in the scientific community and significantly influences recent energy policies [2]. Thanks to the high efficiency attainable, central tower CSP show the major percentage between the plants under development [3]. Although the electricity production can rely on mature technologies such as thermal cycles already used in fossil fuel power plants [4], other parts of the process still need further researches. In particular, a suitable system to store the solar energy [5] is recognized as one of the most important step in order to reach high performances and dispatchable electricity generation. At the state of the art, heat is mostly stored in form of sensible heat by means of molten salts [6]; in this framework Thermo-Chemical Energy Storage (TCES) constitute a promising alternative because of its higher operating temperatures, higher energy density and lower (or null) thermal losses [7]. The reversible reaction that constitutes the Calcium-Looping shows many interesting aspects. The European project SOCRATCES [8] is conducted with the aim of investigating its integration feasibility in a central tower CSP plant. This process includes an endothermic reaction (calcination) in which $CaCO_3$ is converted into CaO and CO_2, and the opposite exothermic reaction, called carbonation.

The recognized CaL integrations with thermal cycles are two: direct and indirect [9]. In the first one, electricity is generated using in the

DOI of original article: https://doi.org/10.1016/j.ecmx.2020.100039
* Corresponding author.
E-mail address: umberto.tesio@polito.it (U. Tesio).

https://doi.org/10.1016/j.ecmx.2020.100038
Received 23 December 2019; Received in revised form 11 February 2020; Accepted 12 February 2020
Available online 20 February 2020
2590-1745/ © 2020 The Authors. Published by Elsevier Ltd. This is an open access article under the CC BY-NC-ND license (http://creativecommons.org/licenses/BY-NC-ND/4.0/).

Nomenclature

Nomenclature and letters

A	Heat exchange area, m^2
$CaCO_3$	Calcium carbonate
CaO	Calcium oxide
CO_2	Carbon dioxide
$\dot{m}$	Mass flowrate, kg/s
n	Moles number
P	Pressure, bar
Q	Heat, J
T	Temperature, K
U	Global heat transfer coefficient, $W/(m^2*K)$
$\dot{W}$	Power flux, W
X	CaO conversion

Abbreviations

B	Blower
BIT	Blower inlet temperature, K
C1IP	First compressor inlet pressure, bar
CaL	Calcium-Looping
CCS	Carbon Capture and Storage
CIT	Compressor inlet temperature, K
CPC	Compound Parabolic Concentrator
CSLTROT	Cold Side LTR Outlet Temperature
CSP	Concentrated Solar Power
HTCW	Heat Transfer at Carbonator Wall
HEN	Heat Exchangers Network
HEX	Heat exchanger
HRCP	Heat Recovery on Carbonator Products
HTR	High Temperature Regenerator
ic	Specific investment cost, $/MJ
IC	Investment cost, $
LTR	Low Temperature Regenerator
RFF	Recompression Flow Fraction
RSP	Recompression Split Position
SC	Storage compressor
sCO_2	Supercritical CO_2
ST	Storage turbine
T1IP	First turbine inlet pressure, bar
TCES	ThermoChemical Energy Storage
TIT	Turbine inlet temperature, K

Greek letters

Δ	Difference
β	Pressure ratio
η	Efficiency
φ	Thermal flux, W

Subscripts and superscripts

0	standard conditions
carb	carbonator
CarbS	Carbonator side
clc	Calciner
ClcS	Calciner side
des	Design
EG	Electricity Generator
el	Electric
eq	Equivalent
H	Heater
helio	Heliostat field
in	Inlet
lm	logarithmic mean
MIN	Minimum
out	outlet
PB	Power Block
r	reaction
tot	Total
un	unreacted

turbine directly the carbon dioxide exiting from the carbonator. In the second type a separate power block is thermally fed by the two hot carbonation products. In this last case, practically any thermodynamic cycle operating in a compatible temperature range can be chosen.

According to scientific literature, direct integration is the most investigated alternative; an overview of this configuration if provided in [10]. A detailed study is performed in [11] and different heat exchanger networks are proposed in [12] for the discharging process. The possibility to store solids at high temperatures is analyzed in [13], while direct integration and indirect integration of an ORC are evaluated in [14]. The indirect integration of a supercritical carbon dioxide (sCO_2) thermal cycle in a CSP plant with TCES based on CaL is investigated in [15] and compared to both direct and indirect integration alternatives. The system performance is penalized by the fact that the power block is non-optimized and, as a consequence, the indirect integration of a less performing Rankine cycle results to be more convenient in energy terms. A detailed review on the Calcium-Looping application as TCES in the CSP field and the state of the art of this technology are provided in [16]. Here is shown the importance of a thermal transfer process optimally performed. The discharging process optimization conduced both at level of process components (turbomachinery and reactors) operating conditions and heat transfer is analyzed in [17] comparing both the integration alternatives and different thermodynamic cycles. The highest efficiency is attained with a supercritical carbon dioxide power block.

On the basis of those energy analysis is possible to say that the sCO_2 cycle indirect integration worth a deep and comprehensive investigation, which is actually lacking in scientific literature; its stand-alone performance can overcome 50% [18] and most of the layouts presented in literature are quite simple, involving a reduced number of components. A detailed review is provided in [19], where more than 40 cycle configurations are presented.

In a previous article (Part 1) the price estimation of the main components is performed to economically analyze the system and to compare in terms of investment cost the most suitable integration options.

The purpose of this work is to make a comprehensive investigation, in efficiency and economic terms, of the Calcium-Looping indirect integration in a central tower CSP plant with a thermal cycle based on supercritical CO_2. Both the cases 1) power block fed with a heat recovery on the carbonation products and 2) direct heat exchange executed at the carbonator walls are evaluated. To perform a complete and coherent analysis it is necessary to use a full optimization framework as the HEATSEP method [20], in which all the heat transfer processes are optimized through the pinch analysis [21] and, at the same time, the process components (reactors, turbines, compressors) and other plant parameters are optimized with a heuristic method. The thermodynamic cycle layout is established during the optimization by a superstructure in order to reach the most favorable configuration for the CaL indirect integration. Simulating the entire CSP plant (from the heliostat field to the electric generator) allows estimating the investment cost and makes possible to execute a multi-objective analysis in order to observe the

effects on the system layout of the economic aspects.

The most important novelties characterizing this work are represented by 1) the depth of the optimization performed for the system layout, heat transfer processes and operating conditions; 2) the evaluation of the thermal transfer at the carbonator wall, which is, according to the present scientific literature, investigated for the first time in this field with this study; 3) the addition of the solar side in the plant simulation; 4) calciner and solar side optimization and dimensioning under transient conditions and 5) the economic optimization performed for a CaL indirect integration in CSP.

The paper is structured as follows:

- Section 2: CaL operation in case of indirect integration is exposed;
- Section 3: plant model and the optimization structure is presented;
- Section 4: economic analysis methodology is discussed;
- Section 5: multi-objective optimization is explained;
- Section 6: results obtained are reported and commented;
- Section 7: final comments and considerations are provided.

2. Case study

A conceptual schematic of the CaL indirect integration is provided in Fig. 1, where are contemporary represented the two alternatives for the power block feeding considered in the analysis:

1) Heat Recovery on Carbonation Products (**HRCP**), when is exploited the sensible heat of carbonator outflows (marked with A in Fig. 1);
2) Heat Transfer on Carbonator Wall (**HTCW**), when the heat of reaction is directly provided to the thermal cycle (marked with B in Fig. 1).

The portion of the plant between the heliostat field and the three storages, the so called calciner side, is devoted to the storage charging; the remaining section is the carbonator side, where discharging process and the electricity production occur.

The CaL process begins when the stream of $CaCO_3$ (and unreacted CaO) is extracted from the storage, preheated and sent to the calciner, where the solar radiation reflected by the heliostat field and concentrated by the Compound Parabolic Concentrator (CPC) drives the endothermic reaction. Because of the presence of an inert gas (steam or helium) in the reactor atmosphere is possible to operate at relatively low temperatures, such as 725 °C–750 °C [10,22]. The advantages are a reduction in the receiver thermal losses and a less demanding configuration in terms of construction materials. The drawbacks are an increase in the plant operation complexity due to the installation of a suitable gas separation unit and an efficiency penalty for its energy consumption. A pure CO_2 reactor atmosphere is therefore assumed and its nominal temperature is set to 950 °C [14].

The solar calciner products, CaO and CO_2, are cooled down and sent to the storages; in order to avoid an excessive vessel dimension, carbon dioxide is compressed up to 75 bar and cooled it down to the ambient temperature [11]. The insertion of intercooling stages allows reducing the compression power, which will be partially recovered during the discharge process, when the stoichiometric CO_2 is heated and expanded up to the carbonator pressure. Once that the recirculated carbon dioxide and the storage carbon dioxide are mixed, the reactants are brought to their carbonator inlet temperature and the exothermic reaction releases the heat previously absorbed. The reactor atmosphere is composed of pure CO_2 and the design temperature is superiorly limited to 875 °C [13]. For both the alternatives of power block feeding (HRCP and HTCW), $CaCO_3$ and CO_2 in excess are cooled down, the solid stream is sent to the storage and the gaseous flow is recirculated in the carbonator side thanks to a fan that compensate the pressure losses occurring in the heat exchangers. As emerges from the process description, the use of external heat sources is intentionally avoided in order to obtain a system exploiting a 100% renewable energy source.

The other works found in literature analyze exclusively the configuration where the thermal power is provided to the power block by the carbonator products (HRCP). In this case, the reactor is expected to have an easier operation since the exothermic reaction is the only process carried out in this component. In this study the second alternative (HTCW) is investigated for the following reasons: i) evaluating the possible efficiency benefits brought by the execution of the carbonation in a non-adiabatic reactor; ii) it is reasonable to expect that the carbonator will operate with a lower CO_2 excess, leading to smaller reactor volumes; iii) moving the power block heat transfer to the carbonator wall simplifies the carbonator side Heat Exchanger Network (HEN) layout. The presence of heat exchangers with a high-pressure power fluid on the reactor wall and the more complex control determined by the higher number of variables characterizing the component operation represent two criticalities for this type of carbonator. However, this kind of reactors are already developed for supercritical Rankine cycles operating with CaL for Carbon Capture and Storage [23] and recent studies included sCO_2 cycles [24].

Regarding the thermodynamic cycle, the importance of evaluating different configurations is evident in the perspective of a multi-objective optimization, where the addition/removal of turbomachinery or heat exchangers influences in opposite ways the plant efficiency and costs. However, the changes occurring in the power block have a noticeable impact both on the carbonator side operation and HEN layout. It is therefore necessary to find a suitable optimization method able to handle the choice of the power block layout, the primary components operating conditions and the heat transfer processes. Optimizing the power block operation and its integration into the Calcium-Looping TCES contemporary is an higher quality option with respect to the one adopted in [17], where the process is divided into two separate steps, allowing to reach a more relevant solution.

Being the carbonator side operation independent with respect to the calciner side, the energy optimization for the indirect integration should be actually performed only on the discharge process [25]. However, to perform

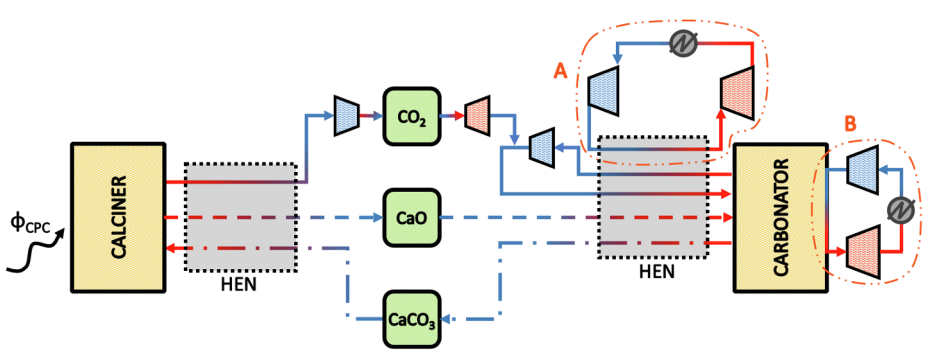

Fig. 1. CaL indirect integration plant layout.

the economic analysis in a similar situation it would be necessary to associate a price to the reactants flows extracted from the storages, which depends both on the solar side and calciner side. For this reason, the plant simulation comprises these two last layout portions, having therefore the solar radiation as single power input.

3. Plant simulation and optimization model

The components simulation and the plant optimization are separately discussed for the different sections in which the CaL system can be divided. Generally speaking, the chemical reactors are simulated with the same energy balance set in [11]; the reaction kinetics is not investigated because is not between the purposes of the present work. The power block and the carbonator side study is conducted for the stationary case, while a simplified transient analysis is chosen to take into account the intrinsic time dependence affecting the solar and calciner sides.

Thermo-physical properties of the involved substances are taken from [26] for CO_2, [27] for CaO and [28] for $CaCO_3$.

To sum up the optimization structure in an as clear as possible way, the entire process is represented in Fig. 2 in form of flow chart. Steps highlighted in orange indicate optimizations performed for process components operating conditions, while blocks in blue are referred to thermal transfer optimizations.

terms of efficiency and costs), the power block is simulated through a superstructure. This is done to avoid running an excessive number of different optimizations for any layout investigated (the possible combinations generate 10 different configurations). A complete configuration, obtained as the sum of the different layouts, is provided to the optimization process and when the algorithm spontaneously tends to impose a null flowrate/pressure drop/temperature difference on a specific component, this is automatically bypassed by the power fluid and therefore eliminated from the layout.

The total superstructure layout is shown in Fig. 3 (LTR/HTR stand for low/high temperature regenerator); the components filled in yellow can be removed during the optimization process, while the dashed lines at the split for the recompression branch indicate that the connection can assume only one between the two alternative positions (0 or 1, as if it was a switch), which determines if the layout is in a precompression configuration rather than in pure recompression. The choice between the layouts considered is made taking into account both cycle performance and topology complexity [32,33].

In Table 1 the assumptions made for the thermodynamic cycle, in accordance to the data found in [29,33–35] are reported; dry cooling with ambient air is assumed for the present analysis. Only three constraints are defined for the power block: 1) imposed the minimum temperature difference between the LTR cold inlet and hot outlet is imposed in order to guarantee the maximum heat recovery on the flow

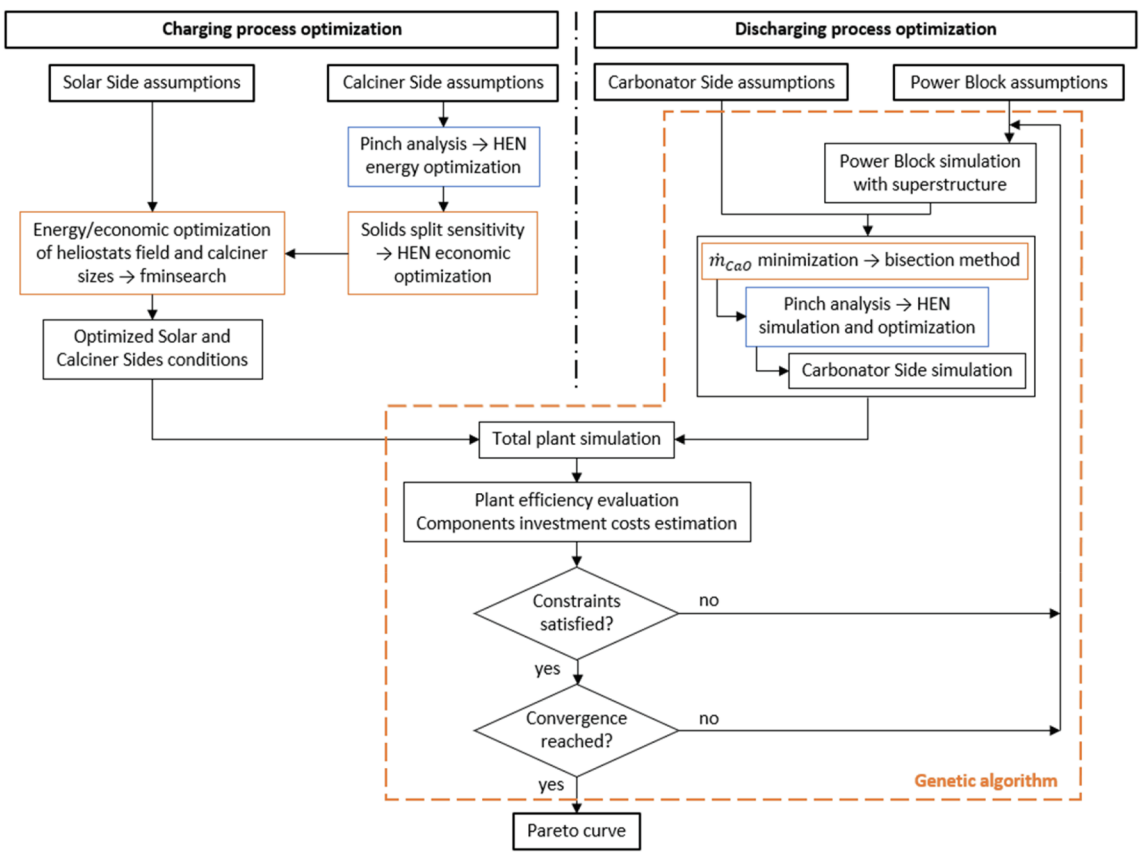

Fig. 2. Schematic of the complete optimization process.

3.1. Power block

The interest for supercritical carbon dioxide cycles in CSP increased significantly during the last years and several layouts are proposed in literature [29–31] showing encouraging performances. The alternatives investigated in the present work start from the simplest configuration (single compressor, turbine, regenerator, heater and cooler) up to the most complex case, which includes reheating, inter-cooling, recompression and pre-compression stages. In order to find the most convenient configuration (both in

exiting the turbine. 2) the second constraint establish that the turbines inlet temperatures are equal. 3) the third one prescribe a net electrical power generation of 2 MW. This last assignment is provided taking into account the early stage of development characterizing this technology and its low value of TRL (Technology Readiness Value). Consequently, it is assumed the system size of a pilot plant.

The independent variables of the optimization are: recompression split position (RSP), first Compressor Inlet Pressure (C1IP), first Turbine

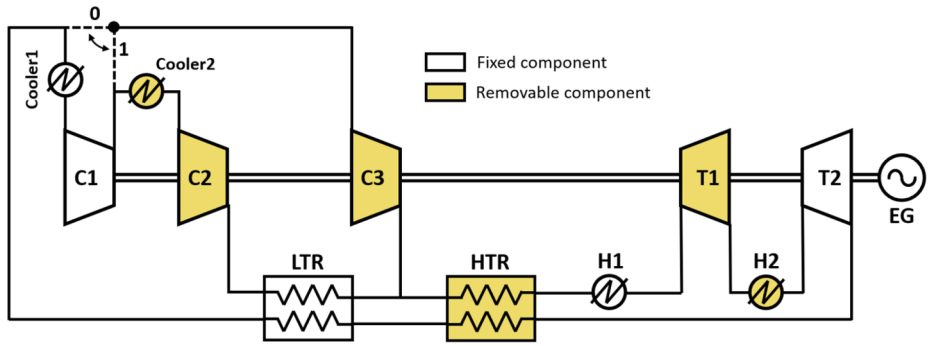

Fig. 3. sCO_2 thermal cycle superstructure.

Table 1
Thermodynamic cycle assumptions.

Parameter	Component/stream	Value
Isentropic efficiency	Turbine	0.92
	Compressor	0.88
Electrical efficiency	Electric generator	0.98
Pressure losses	Regenerator hot side	1.5%
	Regenerator cold side	1%
	Heater	1.5%
	Cooler	2%
Ambient temperature	Air	20 °C
Minimum ΔT	Heater	20 °C
	Cooler	15 °C

Inlet Pressure (T1IP), Recompression Flow Fraction (RFF), Turbines Inlet Temperature (TIT), Cold Side LTR Outlet Temperature (CSLTROT), first compressor pressure ratio (β_{C1}), first turbine pressure ratio (β_{T1}) and minimum temperature difference achievable in the regenerators ($\Delta T_{min,R}$). Is worth to notice that it is possible to exclude CSLTRT from the independent variables in case of isothermal mixing between the two regenerators. In this case, this parameter is assumed as variable to evaluate the possible convenience in mixing the streams at different temperatures, expanding the optimization extent.

The variation ranges adopted for the optimization process are shown in Table 2. Their bounds are fixed according to [33] and [36]. The choice for the optimization method is explained in the next paragraph.

The power block efficiency (η_{PB}) allows to evaluate the thermodynamic cycle performance separately from the rest of the plant: this is calculated with Eq. (1).

$$\eta_{PB} = \frac{\dot{W}_{EG}}{\Phi_{H1} + \Phi_{H2}} \tag{1}$$

where $\dot{W}_{EG}$ is the electric generator output and $\Phi_{H1/2}$ is the thermal flux absorbed by the heaters.

3.2. Carbonator side and storages

The main characteristic of CaL indirect integration is that the gaseous stream in the carbonator side does not act as power fluid, so the CO_2 loop is only affected by the pressure losses occurring in the heat exchangers. As demonstrated in [15], in indirect integrations the use of a pressurized reactor is deleterious in terms of efficiency (although it must be recognized that the reaction kinetics would be enhanced [10]). For this reason, the ambient pressure is imposed as the design value for the carbonator reactor and, as a consequence, the other pressures are directly calculated and fixed for the entire optimization process. An average CaO conversion (X) is provided to completely simulate the carbonation reaction (set equal to 0.5 [15]) such that, for the energy optimization purposes, it is not relevant to establish the reactor type for the energy analysis; however, it is necessary to specify it for the economic analysis, as in the next paragraph.

Several aspects must be taken into account for the carbonator side optimization, such as the operating conditions of process components, the heat exchange between reactants and products and the power block thermal feeding. One of the most appropriate methods to optimize the problem [25] is the HEATSEP, which has been successfully used for different applications in the energy field [37–39]. This methodology uses two different optimization techniques, one for the primary components design parameters (usually a heuristic algorithm) and another for the heat transfer occurring between the involved streams (pinch analysis). These two optimizations are performed contemporary in the model execution and, specifically, the second one is nested into the first one. The Heat Exchanger Network layout remains therefore unknown for the entire problem resolution and it is possible to design it only in the postprocessing phase. In other words, instead of simulating a HEN for the fluids involved in the thermal transfer, "thermal cuts" are inserted in place of the heat exchangers, assuming that all the streams are free to transfer heat between them according to a "black box" approach. A schematic for the approach applied to the considered system is shown in Fig. 4. The stream representing the supercritical CO_2 to be heated up (in yellow) is excluded from the pinch analysis if the configuration of Heat Transfer at the Carbonator Walls is selected (b).

Two advice are found for the HEN design [12]: heat transfer between solids and splits of solid stream should be avoided since their execution is relatively complex in technical terms.

One single heating and expansion stage are considered for the stoichiometric CO_2 extracted from the storage, with the aim of reducing the layout complexity in terms of both thermal transfer and primary component structure. Furthermore, as proposed in [11], it is possible to provide the solid flowrates to the storages at a temperature slightly different than the design value, assuming that the thermal dispersions in the non-insulated vessels after a while make the temperature of solids equal to the environment.

The assumptions for the operation (made according to [10,13,15]) are summed up in Table 3.

Considering the discharging process, the parameters chosen as independent variables for the carbonator side optimization are:

Table 2
Power block independent variables ranges.

Independent variable	Lower bound	Upper bound
RSP	0	1
C1IP	75 bar	95 bar
T1IP	180 bar	250 bar
RFF	0.4	1
TIT	500 °C	700 °C
CSLTROT	100 °C	450 °C
β_{C1}	1	4
β_{T1}	1	4
$\Delta T_{min,R}$	5 °C	20 °C

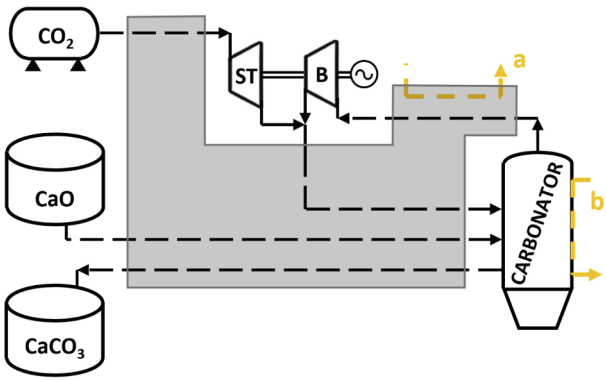

Fig. 4. Carbonator side layout for the HEATSEP optimization method.

Table 3
Carbonator side assumptions.

Parameter	Component/stream	Value
Operation time	Carbonator side	24 h
CaO conversion	CaO	0.5
Thermal losses	Carbonator	1% of reaction heat
Isentropic efficiency	Storage turbine	0.8
	Blower	0.8
Electrical efficiency	Electric generator	0.98
Pressure losses	Mixed CO_2	6%
	Recirculated CO_2	4%
	Storage CO_2	1%
Storage temperature	Storage vessels	20 °C
CO_2 storage pressure	CO_2 vessel	75 bar
Solid conveying electrical consumption	CaO, $CaCO_3$	10 kJ/(kg*100 m)
Storages-carbonator distance	CaO, $CaCO_3$	100 m
Heat rejection electrical consumption	Coolers	0.8% of rejected heat
Minimum ΔT	Gas-gas HEXs Gas-solid HEXs HTF-solid HEXs	15 °C

carbonation temperature (T_{CARB}), CaO carbonator inlet temperature ($T_{CaO,IN}$), CO_2 carbonator inlet temperature ($T_{CO2,IN}$), storage turbine inlet temperature (STIT), blower inlet temperature (BIT) and CaO mass flowrate extracted from the storage ($\dot{m}_{CaO}$). The variation ranges, established according to [15], are reported in Table 4.

More in detail, the optimization is structured as follows: a genetic algorithm generates a population of individuals (i.e. a set of independent variables). The first plant portion to be simulated is the power block, such that its thermal requests is known in terms of temperatures and flow. Then the carbonator side pressures and temperatures are computed, but the flowrates have still to be determined. The configuration evaluated must satisfy the thermal requirement of both the power block and the carbonator side without the use of an external hot source with the minimum reactants consumption (CaO and CO_2). For this purpose a bisection algorithm is adopted, executing iteratively the pinch analysis to obtain the optimal flowrate values for every individual of the population (i.e. a set of independent variables). Once that the first two plant portions are computed, the remaining parts are consequently simulated and the genetic algorithm can evaluate the constraints fulfillment and calculate the objective functions.

From a preliminary run of the complete optimization is observed the tendency to reach a configuration where a small part of the thermal transfer process includes a solid-solid heat exchange, since the hot CO_2 recirculated is not cooled down to a sufficiently low temperature. The addition of a further constraint that prevent a similar possibility is sufficient to overcome this issue and the efficiency penalty occurring is negligible (≈1% in relative terms).

Is worth to notice that the constraint on the minimum temperature difference imposed at the heat exchanger used for the pinch analysis varies depending on the type of flow. The sCO_2 requires a ΔT_{MIN} equal to 20 °C while 15 °C is sufficient for the other flows. In case only one stream requires a ΔT_{MIN} different from all the others, a correction to the calculation of the grand composite curve can be applied to the stream showing the different requirement.

The same strategy is adopted in the cases the solid-solid thermal transfer cannot be avoided (even with the addition of further constraints). This happens when the power block is fed at the carbonator wall. Here the ΔT_{MIN} of the cold solid stream is increased to take into account the presence of a Heat Transfer Fluid. According to the operating temperatures, the choice falls on gases or liquid metals [16], but for the purposes of the present work, the HTF remains unspecified.

As proposed in [17,25], the parameter used to evaluate the discharging process performance is the carbonator side efficiency (η_{carb}), defined as shown in Eq. (2).

$$\eta_{carb} = \frac{\dot{W}_{el(CarbS+PB)}}{\dot{n}_{CaO} X \Delta h_r^0} \tag{2}$$

Terms here appearing are: carbonator side and power block electrical power production ($\dot{W}_{el(CarbS+PB)}$), molar flowrate provided to the reactor ($\dot{n}_{CaO}$), CaO conversion (X) and molar enthalpy of reaction in standard conditions (Δh_r^0).

3.3. Calciner side

The calciner side optimization can be conducted separately from the two sections previously analyzed since any change occurring in the discharging process does not have a direct influence on this plant portion and its operation is only influenced by the solar side. Some simplifying assumptions are made in order to take into account its strictly time dependent functioning. To do that, is necessary to establish the solar calciner typology. The same design considerations made in a previous analysis (Part 1) are again considered in the present analysis: a rotary kiln is assumed as receiver and the same layout obtained from the pinch analysis and solid split optimization is adopted for this plant section.

Once that this plant section is included in the analysis, it is possible to calculate the Calcium-Looping TCES efficiency (η_{CaL}) with Eq. (3), as proposed in [11]; $E_{el,tot}$ stands for the total daily electric energy production and $Q_{clc,net}$ is the thermal flux absorbed at the calciner net of losses.

$$\eta_{CaL} = \frac{E_{el,tot}}{Q_{clc,net}} = \frac{\int_{day} (\dot{W}_{el,CarbS}(t) + \dot{W}_{el,ClcS}(t))dt}{\int_{on}^{off} \eta_{helio}(t)\eta_{CPC}\eta_{clc}A_{helio}DNI(t)dt} \tag{3}$$

3.4. Solar side

The solar side is simulated and optimized through a simplified approach. The winter solstice is set as the nominal day to dimension this plant portion in order to guarantee the power production imposed to the power block even in the most unfavorable day of the year. The plant location, the procedure to evaluate the Direct Normal Irradiation (DNI)

Table 4
Carbonator side independent variables ranges.

Independent variable	Lower bound	Upper bound
T_{CARB}	500 °C	875 °C
$T_{CaO,IN}$	310 °C	860 °C
$T_{CO2,IN}$	35 °C	860 °C
STIT	270 °C	650 °C
BIT	35 °C	400 °C
$\dot{m}_{CaO}$	–	

and the heliostat field hourly efficiency (including atmospheric attenuation, mirrors reflection, shadowing and blocking, spillage and cosine losses) for a north-field arrangement are taken from [40] (DAHAN power plant). The complete and detailed treatment related to this plant section optimization is exposed in Part 1, and identically adopted for this companion study. As discussed in the former study, it is possible to choose between energy or economic optimization for the dimensioning of solar and calciner sides. Therefore, a new independent variable (Charging Process Optimization, CPO) is added in order to take into account this aspect. In this way, for the same amount of $CaCO_3$ daily converted, the convenience between bigger heliostat field and smaller solar calciner or vice versa is evaluated by the algorithm and the most suitable configuration is selected.

4. Economic analysis

The estimation of components investment cost is done with the aim of evaluating the convenience of a plant configuration in economic terms. The cost functions and the methodologies adopted for the estimation of the capital investment are described in Part 1.

The absence of external sources consumption (such as fossil fuels) and the direct proportionality of annual costs (due to operating, maintenance and interest rates) to the total plant cost, allow using the total investment to evaluate the economic affordability of a specific layout configuration.

For the case of power block in HRCP configuration, the reactor is nearly adiabatic (except for the thermal losses due to non-ideal insulation) and its price mainly depends on its volume. The volume is influenced by the inlet volume flowrates and their residence time. For this reason, the investment cost function adopted in this configuration is referred to an entrained flow reactor, and the reactants volume is used as scaling parameter.

Concerning the option of thermal transfer directly performed on the carbonator wall, the reactor cost increases significantly because of the presence of heat exchangers for the power fluid at high pressure. The heat released during the exothermic process is directly proportional to the thermal flux provided to the power block and therefore it can be used as scaling parameter for this kind of component, as appears in the cost function for a fluidized bed carbonator.

As already explained in the previous section, using the HEATSEP method to optimize the carbonator side thermal transfer process does not require to provide a Heat Exchanger Network for this plant section, which is designed in the post-processing phase. However, for the economic optimization purposes, the HEN cost has to be provided to obtain an as complete as possible evaluation. A parameter is selected in order to link the composite curves of the pinch analysis with the corresponding HEN price; this is done such that its estimation can be performed during the optimization process. This parameter is the equivalent product between the global heat transfer coefficient and the heat transfer area (UA_{eq}), computed with a summation on all the segments composing the hot and cold composite curves (Eq. (4)). The strategy developed to overcome this issue is the following: 1) some interesting cases are simulated in a preliminary run; 2) for those the Heat Exchanger Network is synthetized; 3) the investment costs are computed and 4) UA_{eq} is evaluated.

$$UA_{eq} = \sum_i \left[\frac{\phi_i}{\Delta T_{im,i}} \right] \tag{4}$$

A cost function for the carbonator side HEN is therefore easily derived performing a data fit on the results obtained and implemented in the optimization algorithm. The term used as scaling parameter is the UA_{eq}, such that, although during the network layout is unknown during the process, it can be estimated computing a benchmark from the pinch analysis. Two different functions must be developed for the cases of HRCP and HTCW because of the consistent differences occurring in their final layout (and therefore in their price).

Another parameter assumed as independent variable of the optimization process is the number of intercoolings performed for the CO_2 compression in the calciner side. In this way, the energy benefits and the economic penalties occurring in case of an increasing number of stages (the maximum is set equal to 5 [13]) are both considered and the algorithm is free to establish the most convenient alternative.

Finally, the independent variables assumed for the optimization process are summed up in Table 5.

5. Multi-objective optimization

The economic analysis is in contrast with the energy optimization, since minimizing the investment cost leads to less performing configurations. It is therefore interesting to evaluate possible compromises between these two aspects and observe how determined options affect the solution to which the optimization process converges.

For the energy optimization, the objective function is the total plant efficiency (η_{tot}) referred to the design day, defined in Eq. (5):

$$\eta_{tot} = \frac{E_{el,tot}}{Q_{sol}} = \frac{\int_{day} (\dot{W}_{el,CarbS}(t) + \dot{W}_{el,ClcS}(t))dt}{\int_{day} A_{helio} DNI(t)dt} \tag{5}$$

The terms appearing in the calculation are: daily net electrical energy ($E_{el,tot}$), daily solar energy (Q_{sol}), net power production/absorption at carbonator/calciner side ($\dot{W}_{el,CarbS/ClcS}$), total heliostats area (A_{helio}) and Daily Normal Irradiation (DNI).

The objective function for the economic optimization is the specific plant investment cost (ic_{tot}), defined as the total system price normalized by the daily electrical production, as reported in Eq. (6) (where IC_i stands for the i-component investment cost.

$$ic_{tot} = \frac{\sum_i [IC_i]}{E_{el}} \tag{6}$$

6. Results

As already mentioned, the calciner side layout and design parameters are optimized separately from the carbonator side and power block. For this reason, the resulting configuration for charging and discharging plant sections are individually exposed in this paragraph. In addition, the cases of energy, economic and multi-objective optimizations are distinguished and separately presented.

Table 5
Independent variables to be optimized.

	Independent variables								
Power Block	RSP	C1IP	T1IP	RFF	TIT	CSLTROT	β_{C1}	β_{T1}	$\Delta T_{min,R}$
Carbonator Side	T_{CARB}	$T_{CaO,IN}$	$T_{CO2,IN}$	STIT	BIT	$\dot{m}_{CaO}$	HRCP/HTCW		
Calciner and Solar Side	#IC	CPO							

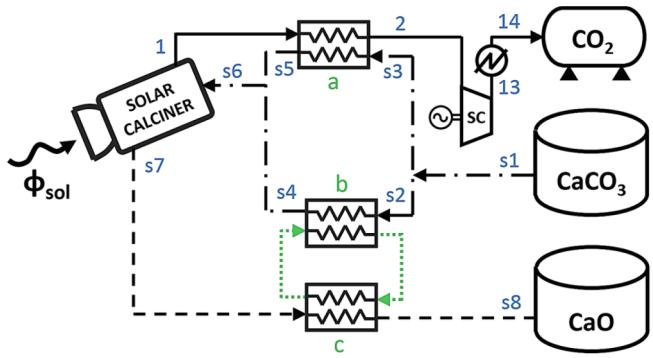

Fig. 5. Calciner side optimized layout.

The results obtained are referred to the plant size investigated in the present study (2 MW_e). These data can be useful for extrapolation of results for systems with higher sizes, but with some limitations. In fact, the exploitation of better performing turbomachinery (higher isentropic efficiency) and more complex layouts (higher number of intercooling/reheating stages) are two aspects influencing both performances and costs of plants with higher sizes that must be properly considered. These elements cannot be included in a simple extrapolation, whose relevance would therefore decrease since resulting as poorly reliable. A complete analysis must be therefore performed to include those important aspects.

However, a suitable way to obtain a reasonable extrapolation of specific investment cost in case of scale-up processes (for the same layout) is proposed in Part 1 of the present analysis.

6.1. Calciner side optimization results

The only variable related to this plant section, that is included in the HEATSEP optimization, is the number of intercooling stages performed during the compression of the carbon dioxide. However, this parameter reaches its maximum achievable value for every configuration obtained from the optimization process. As a consequence, a single calciner side layout is found in the multi-objective optimization, and all the components are simply scaled according to the design flowrates (which are referred to the case of maximum power absorbed at the solar calciner). Fig. 5 shows the resulting configuration; for simplicity, the intercooled compression is not completely represented and in its place is shown a single step Storage Compressor (SC). The operating conditions independent from the specific case analyzed (temperatures and pressures) are reported in Appendix A, while the design flowrates and HEXs nominal thermal powers are presented in the corresponding discharge process results.

Table 6
Main benchmarks for the energy optimized indirect integration.

η_{PB}	η_{CarbS}	η_{CaL}	η_{tot}
52.96%	51.26%	40.44%	20.98%
ic_{tot} [$/MJ]	IC_{tot} [M$]	$\Phi_{des,clc}$ [MW_t]	A_{helio} [m^2]
179.5	29.83	24.88	39,499

6.2. Energy optimization results

The carbonator side and power block layouts obtained from the energy optimization are shown in Fig. 6, while the main benchmarks to evaluate the plant performance are reported in Table 6. The thermodynamic cycle attains its highest efficiency thanks to the various improvements included by the superstructure (intercooling, recompression and reheating) and the heat recovery performed by its regenerators. Both benefits and drawbacks are brought by reaching the HTCW configuration for the power block feeding and the condition of null recirculated CO_2 mass flow rate. The carbonator HEN topology takes advantage from the disappearance of the gaseous carbonator outflow and the number of process components decreases since the carbon dioxide blower is not anymore needed. However, being the solid stream of $CaCO_3$ (and unreacted CaO) the only hot carbonator outflow, heat transfer between solids cannot be avoided for the inlet CaO preheating, making necessary the use of a heat transfer fluid and two HEXs instead of one.

The hot and cold composite curves (a) and the grand composite curve (b) obtained with the pinch analysis for the carbonator side heat recovery are shown in Fig. 7. Being the sCO_2 heaters not included, the thermal flux exchanged between hot and cold fluids is around one third with respect to the case of power block fed with a heat recovery on the reactor outflows.

Concerning the investment costs, in Fig. 8a the main components prices divided by their corresponding plant section are reported. As expected, turbomachinery constitute the major cost in the power cycle, while chemical reactors are definitely the components with highest costs for the carbonator and calciner side, overcoming of one order of magnitude the other devices. In particular, despite the carbonator size is smaller with respect to the solar calciner, the carbonator is more expensive. This is due to the presence of sCO_2 heat exchangers on the reactor walls, which contributes to increase its cost but, at the same time, determines a reduction of the investment needed for the carbonator side Heat Exchanger Network. The contribute to the total investment cost brought by the different plant portions is reported in Fig. 8b; the solar side (heliostat field and central tower) is the most expensive section, reaching the 38% of the total cost. Power block, carbonator side and calciner side have approximately the same

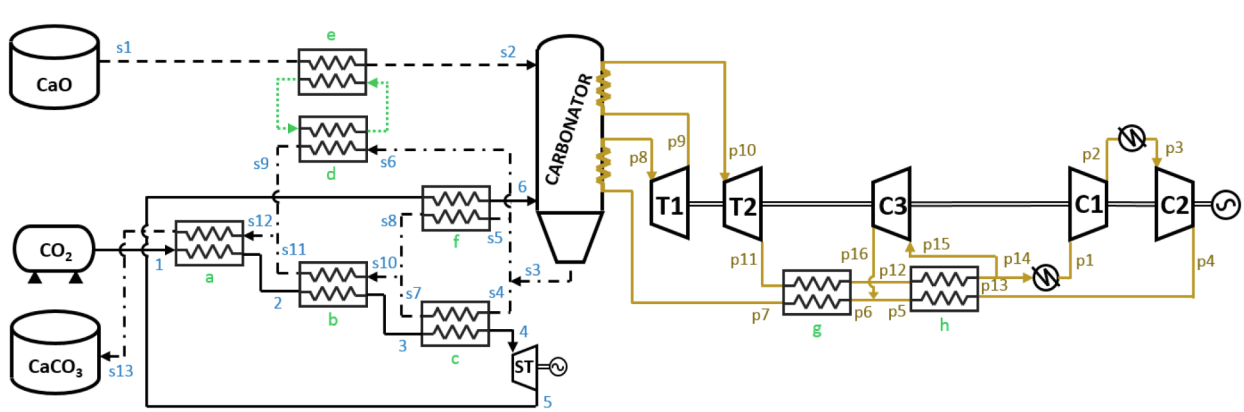

Fig. 6. Carbonator side and power block layout obtained with energy optimization.

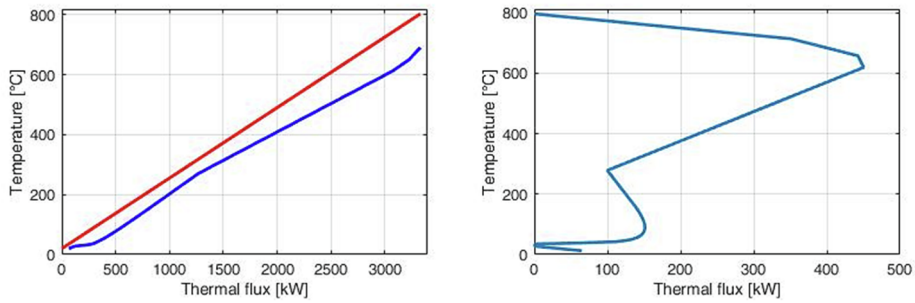

Fig. 7. Hot and cold composite curves (a) and grand composite curve for the carbonator side energy optimization.

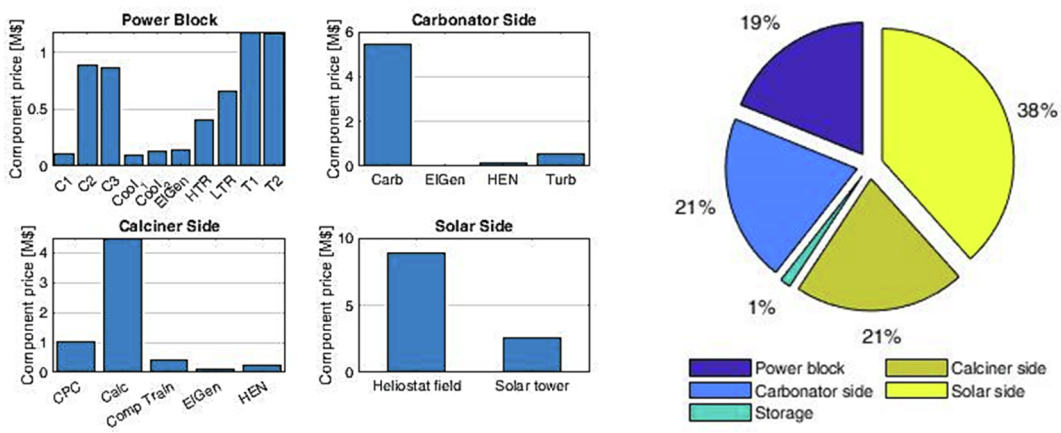

Fig. 8. Components investment cost (a) and total plant investment percentages (b) for energy optimization.

weight; the thermodynamic cycle cost is increased by the improvements adopted such that it constitutes one fifth of the plant investment. Being only composed by the CO_2 vessel, the cost associated to the storage unit appears by far as the less significant between the other plant sections. Plant operating conditions and nominal powers of turbomachinery and heat exchangers are reported in Appendix B.

6.3. Economic optimization results

The layout of carbonator side and power block resulting from the economic optimization are presented in Fig. 9. The thermodynamic cycle reaches a configuration much simpler than the one found in the previous case, but the layout complexity of carbonator side increases. This is because of the presence of CO_2 recirculated and HRCP configuration for power block thermal feeding. Furthermore, the entire thermal transfer process is conduced avoiding heat exchange between solids. Differently from results obtained in [13], both the $CaCO_3$ and the CO_2 exiting the carbonator are used to heat up the supercritical carbon

Table 7
Main benchmarks for the economically optimized indirect integration.

η_{PB}	η_{CarbS}	η_{CaL}	η_{tot}
45.23%	42.76%	32.08%	16.28%
ic_{tot} [$/MJ]	IC_{tot} [M$]	$\Phi_{des,clc}$ [MW_t]	A_{helio} [m^2]
161.2	25.55	28.76	48,764

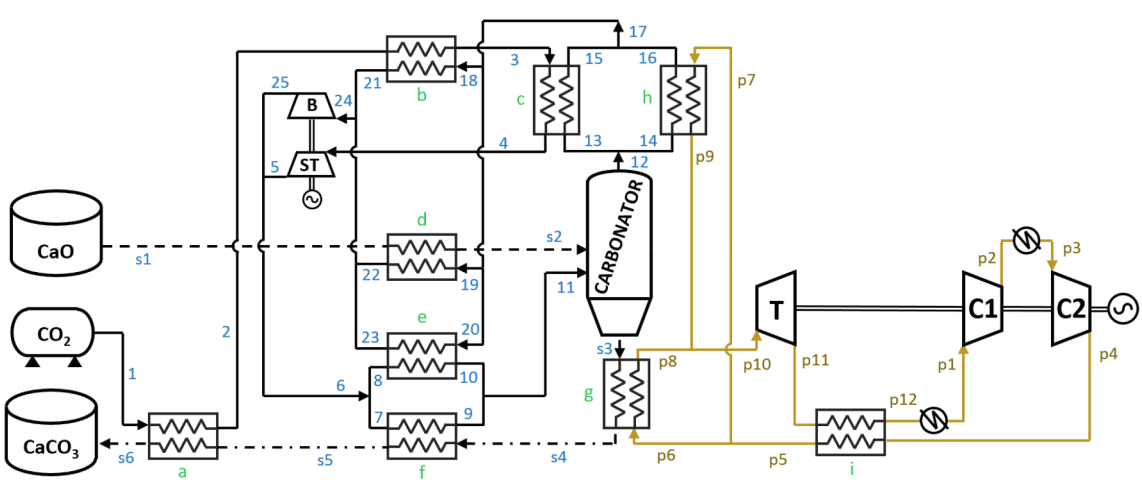

Fig. 9. Carbonator side and power block layout obtained with economic optimization.

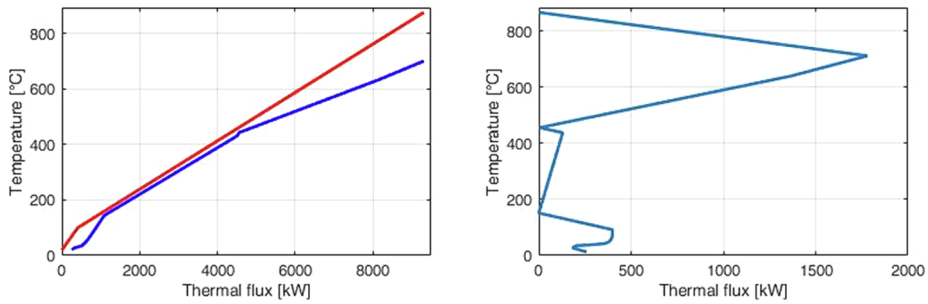

Fig. 10. Hot and cold composite curves (a) and grand composite curve for the carbonator side economic optimization.

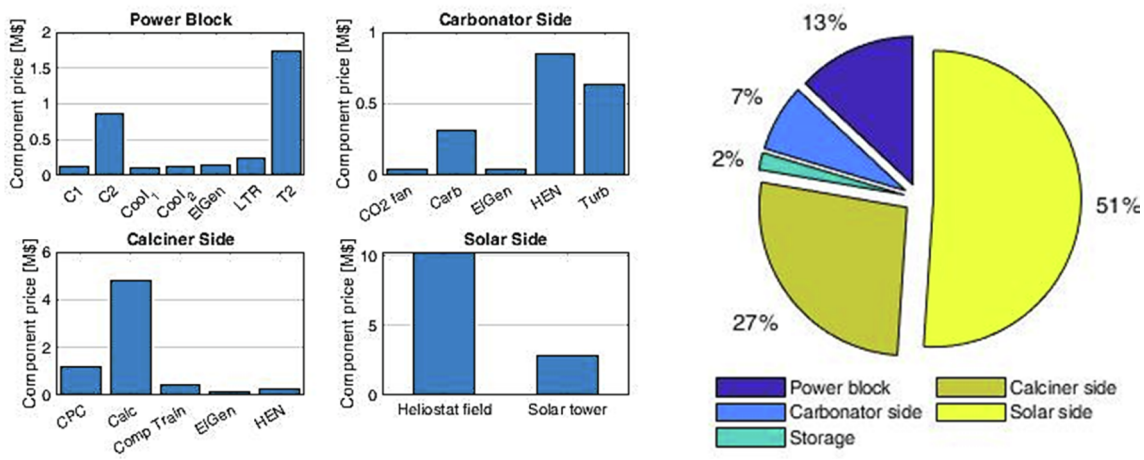

Fig. 11. Components investment cost (a) and total plant investment percentages (b) for economic optimization.

dioxide, leading to a more performing configuration.

Table 7 presents the most important data related to this configuration; the power block efficiency decreases with respect to the previous result (nearly 15% in relative terms) and becomes even worse considering the entire Calcium-Looping process (more than 20%) because of the lower quality mechanism adopted for the thermal cycle feeding.

Hot and cold composite curves (a) and grand composite curve (b) resulting from the pinch analysis are shown in Fig. 10. In order to improve as much as possible the thermal transfer process, the algorithm converges to a configuration with two pinch points: one at low temperature (around 150 °C) and another at high temperature (more than 450 °C). Those are respectively determined by the mixed carbon dioxide and by the supercritical CO_2. Heat at high temperature (above the second pinch point) is devoted to the power block feeding, except for a small part provided to the stoichiometric carbon dioxide.

As possible to observe in Fig. 11, the economic analysis results are quite different with respect to the configuration obtained from the energy optimization. For the same thermal cycle electrical output, a lower efficiency during the discharging phase (power block and carbonator side) determines an increase in the size of the plant sections devoted to the storages charge. Being these the most expensive portions of the system, a reduction in the discharging process could seem as disadvantageous both in energy and economic terms. However, there are two aspects that must be taken in consideration. At first, a lower number of components involved in the thermodynamic cycle reduces its investment cost thanks to the price functions based on power laws. Secondly, passing from a carbonator that exchange heat on its walls to an adiabatic reactor brings particularly significant benefits in terms of component investment cost. Those two phenomena are capable to counter balance the costs rise occurring in the calciner and solar sides, leading to a configuration where less efficient discharging process results economically favorable. As a result, the cost of solar and calciner sides represent more than three fourth of the total plant investment, while the system sections devoted to the discharging process is helved with respect to the configuration obtained from the energy optimization. Also for this case, additional data are provided in Appendix C.

6.4. Multi-objective optimization results

The most important results obtained from the multi-objective optimization are summed up in the Fig. 12. The Pareto curve appears discontinuous because of the changes occurring in the plant layout, achieved by the superstructure and the genetic algorithm. The cases in which the system configuration evolves through the feasible alternatives are represented in the same graph. The highest efficiency is obtained, as expected, when all the thermal cycle layout improvements are adopted (recompression branch, double expansion with reheating and intercooled compression) and the power block feeding is in HTCW configuration. For the same energy output, although a higher plant performance entail a smaller heliostat field (which is the most relevant contribute in economic terms), these arrangements bring a penalty to the components investment cost. In particular, the carbonator price in case of cooled chemical reactor undergoes a significant increase with respect to the adiabatic case. Both in case of HTCW or not, the addition of a reheating stage allows reaching the highest performance, while the intercooled compression is present along the whole Pareto curve. It is important to notice that, in case of recompression cycle, the algorithm never converges to the configuration of precompression (or precooling) but the pure recompression in always preferred. Finally, the most convenient solution in economic terms is also the simplest in terms of power block layout complexity.

The trend of the independent variable values is represented in Fig. 13 (normalized for the respective variation range) along the Pareto

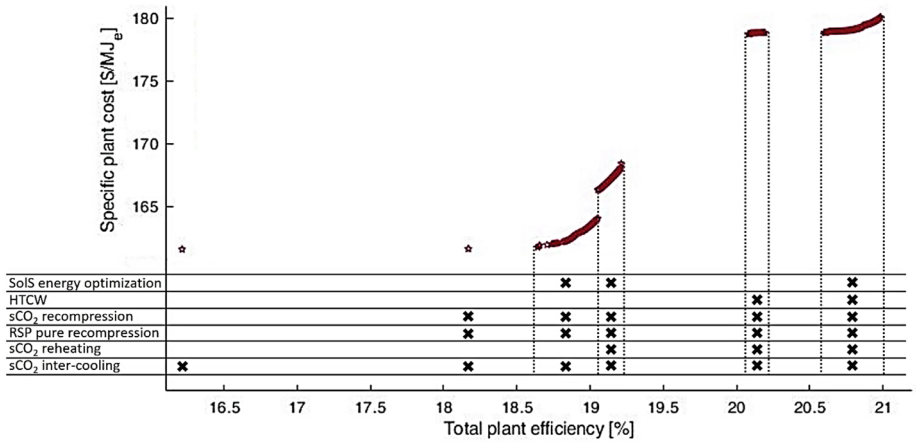

Fig. 12. Pareto curve for the multi-objective optimization.

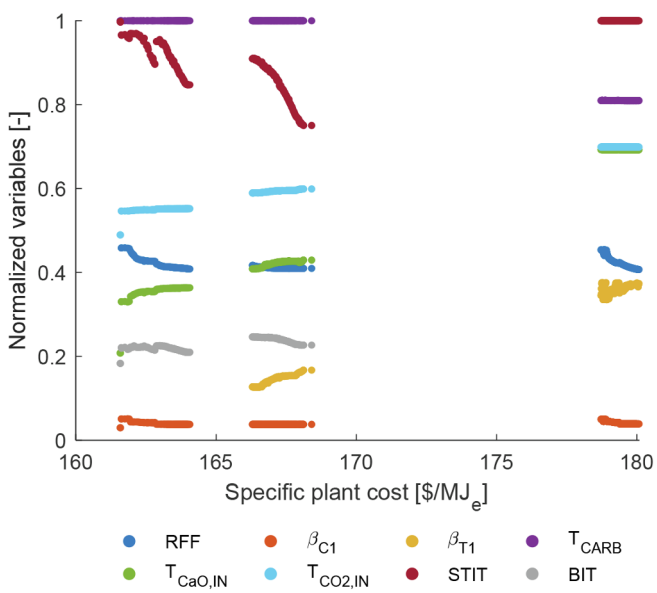

Fig. 13. Normalized variables trends in multi-objective optimization.

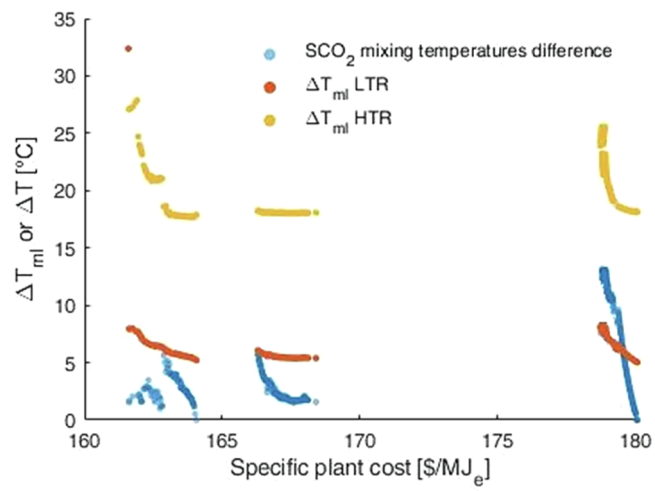

Fig. 14. Heat recovery in the sCO$_2$ thermal cycle.

curve. The number of inter-coolings occurring in the calciner side compression, the power block turbine inlet temperature and pressure always closely approach their maximum, while the C1IP and the $\Delta T_{min,R}$ always converges in a nearby of their minimum. This is why these parameters are not included in the figure.

The plant efficiency is enhanced when the two reactants entering the carbonator undergo a more significant preheating, while the Storage Turbine Inlet Temperature reaches higher values for a less performing power cycle, in order to extract more power from the pressurized stoichiometric CO_2, whose flowrate tends to increase.

There are three aspects occurring in case of HTCW that is worth to mention: first, the carbonator side operating parameters remain nearly constant and only the power block variables are observed to change. This behavior is actually reasonable: in fact, the power cycle integration into the carbonator side has a smaller impact since the thermal flux released to the power block is directly provided by the chemical reaction and not by a thermal recovery performed on the carbonation products. For second, the sensible heat contained in the reactor outflows is exclusively exploited for the inlet streams preheating, and the STIT can maintain its maximum value since heat at high temperature is not devoted to the thermodynamic cycle feeding. The last aspect to mention is that the carbonation temperature does not reach its maximum achievable value, in contrast with the tendency encountered both in this work and in the literature [15] in case of HRCP. This phenomenon presents interesting consequences; in fact, being the carbonation an exothermic reaction, lower temperatures increase the reaction kinetics (according to the chemical equilibrium law), especially in case of a non-pressurized reactor [10]. This leads to shorter residence times and therefore smaller reactor volumes, simplifying the plant operation and reducing (at least theoretically) the carbonator cost.

It is interesting to notice that the CO_2 Blower Inlet Temperature never reaches its minimum value. In fact, being the requested pressure raise low (around 0.1 bar), the energy penalty occurring is not significant; on the other side, the heat exchange process takes advantage form this phenomenon because, when mixed with the stoichiometric carbon dioxide, the total gaseous carbonator inlet requires a lower preheating.

Concerning the sCO$_2$ regenerators, Fig. 14 shows the variation of mean logarithmic temperature difference of LTR and HTR. When the Low Temperature Regenerator reaches a ΔT_{ml} equal to 5, the minimum achievable temperature difference is attained on both the HEX sides, requiring the highest heat transfer surface and component investment cost; its importance in terms of plant performance is therefore fundamental. At the same time is significant to notice that, in order to reach the maximum efficiencies (both in case of HTCW or not), the mixing of the recompressed flowrate occurring between the regenerators becomes isothermal, in accordance to the exergy theory prescriptions.

Finally, in Fig. 15 are reported some other important parameters that affect the plant operation. In case of absence of HTCW, the storage

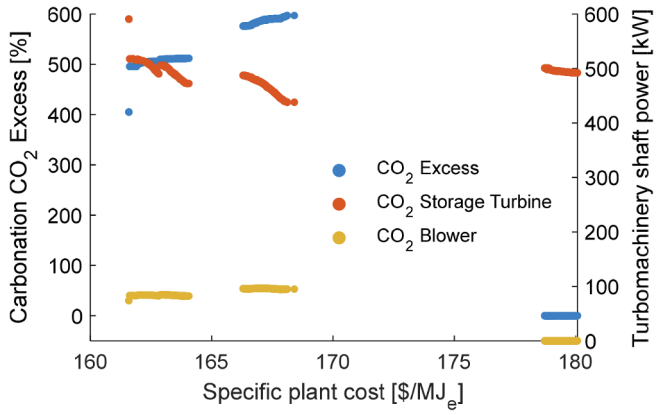

Fig. 15. Carbonation CO2 excess and carbonator side turbomachinery for multi-objective optimization.

turbine shaft power is mainly influenced by its inlet temperature while the blower power follows the trend presented by the recirculated CO_2 mass flowrate. For the same carbonation temperature, the carbon dioxide excess provided to the reactor follows strictly the behavior of two reactants inlet temperatures behavior. An interesting result is obtained in case of HTCW, when algorithm converges to configurations with a CO_2 excess equal to zero and the reaction is therefore carried out in its stoichiometric proportions. This phenomenon leads to a layout simplification, since the mass flowrate of carbon dioxide recirculated becomes equal to zero and there is no need for the blower.

7. Conclusions

As a development of the preliminary analysis performed in the companion paper (Part 1), a comprehensive study of the indirect integration in a CSP plant with TCES based on Calcium-Looping is executed for a Brayton-Joule cycle fed by supercritical carbon dioxide. Both the methodology and the system investigated are novel for this kind of technology. A continuous discharging process is set with an electrical output equal to 2 MW. The integration is conceive such that there is no need for addition of heaters (100% renewable plant). The system optimization is performed both at the level of operating conditions and heat transfer occurring between the involved streams thanks to the adoption of the HEATSEP methodology. This technique uses genetic algorithm, pinch analysis and bisection as optimization methods nested between them. Several power block layouts are considered in form of superstructure and the alternative of feeding the thermodynamic cycle on the carbonator wall or with the reactor outflows are both evaluated. The calciner side is modelled as time dependent and the solar side is included in the analysis; both these plant sections are simulated and optimized as exposed in Part 1. A multi-objective optimization is executed in order to investigate the sCO_2 cycle indirect integration from an energy and economic perspective. Thermal exchange between solids is overcome taking into account the use of heat transfer fluid and the choice between energy or economic optimization for the heliostat field and solar calciner dimensioning is left to the algorithm.

The total plant performance takes consistent advantage from power cycle improvements (intercooling, recompression and reheating) and heat transfer at the carbonator walls, reaching a relatively simple layout with a carbonation temperature not close to the equilibrium. The range of system efficiencies obtained is 16.3–21%. In case of energy optimization, the total system performance is around 21% and the Calcium-Looping process attains 40.4%. The discharging process effectiveness (carbonator side efficiency) reaches 51.3%. This is a satisfactory result when compared to value available in the literature (45–47%) [25].

In case of economic optimization the algorithm converges to a configuration that involves an adiabatic carbonator and a much more basic thermal cycle. This happens since allows reducing the costs associated to the discharging process. More complex (but efficient) power blocks will result convenient only if the prices associated to sCO_2 turbomachinery decrease. This occur in case the technology diffusion reaches the commercial stage. As a consequence, the solar and calciner side costs undergo an increase of 2.2 M$ that is completely covered by the power block and carbonator side investment reduction, equal to 6.6 M$. Passing from the energy to the economic optimization result, the total efficiency decreases (in relative terms) of 22.4%, in the face of a specific plant cost reduction equal to 10.3%. Observing the Pareto curve is possible to say that the introduction of a reheating stage and HTCW in the discharging process are the improvements with a high impact on the plant investment. On the other hand, the addition of a recompression branch in the sCO_2 cycle have good effects on the global efficiency without causing noticeable differences in the system cost. Furthermore, reaching high temperatures and pressures (700 °C, 250 bar), besides the insertion of an intercooling step, results always favorable.

Regarding the Heat Exchanger Networks obtained for the carbonator side, comparing them with the integration presented in [15] for a recompression sCO_2 power block (7 HEXs without taking into account regenerators), it is possible to say that the complexity of their layout is acceptable. In case of minimum investment cost there are 8 heat exchangers, while in case of maximum efficiency are present 6 HEXs plus the carbonator wall that participates to the heat transfer process. The main differences with respect to the study available in literature are that: i) the use of external energy sources is not considered; the power block is fed exchanging heat with both the gaseous and solids stream, enhancing the heat transfer process efficiency.

In conclusion, the complete system modelling and optimization are performed, allowing comparisons with the direct integration alternative and highlighting the most important parameters for the plant operation. Results obtained with the present analysis can be useful for further possible analysis involving other types of indirect integrations or intermediate conditions with respect to the ones assumed in the present work, such as power block feeding simultaneously based on sensible and reaction heat.

CRediT authorship contribution statement

U. Tesio: Conceptualization, Methodology, Visualization, Writing - original draft, Writing - review & editing. **E. Guelpa:** Conceptualization, Methodology, Formal analysis. **V. Verda:** Conceptualization, Methodology, Project administration, Funding acquisition.

Declaration of Competing Interest

The authors declare that they have no known competing financial interests or personal relationships that could have appeared to influence the work reported in this paper.

Acknowledgement

This work has been conducted within the European Project SOCRATCES (SOlar Calcium-looping integRAtion for Thermo-Chemical Energy Storage) GA 727348.

Appendix

A - Calciner side optimization results

	s1	s2	s3	s4	s5	s6	s7	s8	1	2	3	4	5	6	7	8	9	10	11	12	13	14
P [bar]	–	–	–	–	–	–	–	–	1	1	2.1	2	4.2	4.2	8.7	8.6	17.9	17.7	36.8	36.5	75.8	75
T [°C]	20	20	20	841.2	878.9	853.2	950	50	950	35	109.5	35	101.6	35	100.7	35	100.8	35	101.3	35	101.6	35

	Flowrate split
s2	68.0%
s3	32.0%

B - Energy optimization results

	P [bar]	T [°C]	$\dot{m}$ [kg/s]		P [bar]	T [°C]	$\dot{m}$ [kg/s]		P [bar]	T [°C]	$\dot{m}$ [kg/s]
s1	–	20	2.94	s13	–	35	4.09	p6	256.1	195.7	14.93
s2	–	690.9	2.94	1	75	20	1.15	p7	253.5	578.1	14.93
s3	–	803.6	4.09	2	74.75	45.3	1.15	p8	249.7	700	14.93
s4	–	803.6	1.02	3	74.5	246.5	1.15	p9	142.5	621.3	14.93
s5	–	803.6	0.82	4	74.25	650	1.15	p10	140.4	700	14.93
s6	–	803.6	2.25	5	1.11	270.9	1.15	p11	80.1	622.7	14.93
s7	–	285.9	1.02	6	1.04	611.5	1.15	p12	78.9	200.8	14.93
s8	–	285.9	0.82	p1	76.2	35	9.62	p13	77.7	79.8	14.93
s9	–	50	2.25	p2	85.1	42.2	9.62	p14	77.7	79.8	5.31
s10	–	285.9	1.84	p3	83.4	35	9.62	p15	77.7	79.8	5.31
s11	–	130	1.84	p4	258.7	74.8	9.62	p16	256.1	195.7	5.31
s12	–	86	4.09	p5	256.1	195.7	9.62				

Turbomachinery design powers				Discharging plant HEXs design powers			Calciner side HEXs design powers		
$\dot{W}_{T1}\,[kW]$	1407	$\dot{W}_{C2}\,[kW]$	444.4		**Power [kW$_t$]**	**UA [kW/K]**		**Power [kW$_t$]**	**UA [kW/K]**
$\dot{W}_{T2}\,[kW]$	1384	$\dot{W}_{C3}\,[kW]$	431.8	a	216	8.3	a	4654	150.6
$\dot{W}_{C1}\,[kW]$	31.9	$\dot{W}_{ST}\,[kW]$	492.2	b	298	5.0	b	9472	427.5
Daily auxiliaries consumptions				c	546	6.5	c	9472	427.5
$E_{conv}\,[MJ_e]$	$1.22{\cdot}10^4$	$E_{hr}\,[MJ_e]$	$1.89{\cdot}10^3$	**d**	1759	56.3			
Calciner side design flowrates				e	1759	56.3			
$CaCO_3$ + CaO_{un} [kg/s]		16.1		f	444	6.4			
CaO [kg/s]	11.5	CO_2 [kg/s]	4.6	g	7344	405.8			
				h	3415	683.0			

C - Economic optimization results

	P [bar]	T [°C]	$\dot{m}$ [kg/s]		P [bar]	T [°C]	$\dot{m}$ [kg/s]		P [bar]	T [°C]	$\dot{m}$ [kg/s]
s1	–	20	3.51	10	1.04	430.6	1.79	24	1	99.8	5.61
s2	–	448.6	3.51	11	1.04	430.6	6.99	25	1.11	177.6	5.61
s3	–	875	4.89	12	1.04	875	5.61	p1	76.6	35	13.69
s4	–	464.3	4.89	13	1.04	875	0.65	p2	82.9	40.1	13.69
s5	–	158.9	4.89	14	1.04	875	4.96	p3	81.3	35	13.69
s6	–	70.5	4.89	15	1.02	463.8	0.65	p4	255.2	81.5	13.69
1	75	20	1.38	16	1.02	464.2	4.96	p5	252.6	443.8	13.69
2	74.75	144	1.38	17	1.02	464.1	5.61	p6	252.6	443.8	6.53
3	74.5	448.6	1.38	18	1.02	464.1	1.38	p7	252.6	443.8	7.16
4	74.25	632.6	1.38	19	1.02	464.1	2.67	p8	248.8	700	6.53
5	1.11	270.9	1.38	20	1.02	464.1	1.56	p9	248.8	700	7.16
6	1.11	143.9	6.99	21	1	158.9	1.38	p10	248.8	700	13.69
7	1.11	143.9	5.20	22	1	34.8	2.67	p11	79.3	546.1	13.69
8	1.11	143.9	1.79	23	1	158.9	1.56	p12	78.1	86.5	13.69
9	1.04	430.6	5.20								

Turbomachinery design powers				Discharging plant HEXs design powers			Calciner side HEXs design powers		
$\dot{W}_T\,[kW]$	2485	$\dot{W}_B\,[kW]$	73.5		**Power [kW$_t$]**	**UA [kW/K]**		**Power [kW$_t$]**	**UA [kW/K]**
$\dot{W}_{C1}\,[kW]$	32.1	$\dot{W}_{ST}\,[kW]$	575	a	454	15.5	a	5374	173.9
$\dot{W}_{C2}\,[kW]$	435			b	479	31.5	b	10,944	494.0
Daily auxiliaries consumptions				c	304	3.7	c	10,944	494.0
$E_{conv}\,[MJ_e]$	$1.45{\cdot}10^4$	1301	$2.27{\cdot}10^3$	**d**	1301	58.9			
Calciner side design flowrates				e	538	23.4			
$CaCO_3$ + CaO_{un} [kg/s]		18.6		f	1564	67.7			
CaO [kg/s]	13.4	CO_2 [kg/s]	5.2	g	2105	29.2			
				h	2310	32.1			
				i	7354	228.1			

References

[1] SunShot Initiative – Solar Energy Technologies Office – U.S. Department of Energy, Tackling Challenges In Solar: 2014 Portfolio, 2014.
[2] International Energy Agency, Market Report Series: Renewables 2018, 2018.
[3] Palacios A, Barreneche C, Navarro M, Ding Y. Thermal energy storage technologies for concentrated solar power – a review from a materials perspective. Renew Energy 2019.
[4] Stein W, Buck R. Advanced power cycles for concentrated solar power. Sol Energy 2017;152:91–105.
[5] Pelay U, Luo L, Fan Y, Stitou D, Rood M. Thermal energy storage systems for concentrated solar power plants. Renew Sustain Energy Rev 2017;79:82–100.
[6] González-Roubaud E, Pérez-Osorio D, Prieto C. Review of commercial thermal energy storage in concentrated solar power plants: Steam vs. molten salts. Renew Sustain Energy Rev 2017;80:133–48.
[7] Zsembinszki G, Solé A, Barreneche C, Prieto C, Fernández I, Cabeza L. Review of reactors with potential use in thermochemical energy storage in concentrated solar power plants. Energies 2018;11(2358).
[8] Socratces Project | Energy Storage Technologies Viable & Sustainable, [Online]. Available: https://socratces.eu/. [Accessed 2019].
[9] Bioazul, Deliverable D8.1 - First Innovation Evaluation report, 2018.
[10] Ortiz C, Valverde J, Chacartegui R, Perez-Maqueda L. Carbonation of limestone derived CaO for thermochemical energy storage: from kinetics to process integration in concentrating solar plants. ACS Sustainable Chem Eng 2018;6:6404–17.
[11] Chacartegui R, Alovisio A, Ortiz C, Valverde J, Verda V, Becerra J. Thermochemical energy storage of concentrated solar power by integration of the calcium looping process and a CO2 power cycle. Appl Energy Jul. 2016;173:589–605.
[12] Alovisio A, Chacartegui R, Ortiz C, Valverde J, Verda V. Optimizing the CSP-calcium looping integration for thermochemical energy storage. Energy Convers Manage Mar. 2017;136:85–98.
[13] Ortiz C, Romano M, Valverde J, Binotti M, Chacartegui R. Process integration of calcium-looping thermochemical energy storage system in concentrating solar power plants. Energy Jul. 2018;155:535–51.
[14] Karasavvas E, Panopoulos K, Papadopoulou S, Voutetakis S. Design of an integrated CSP-calcium looping for uninterrupted power production through energy storage. Chem Eng Trans 2018;70:2131–6.
[15] Ortiz C, Chacartegui R, Valverde J, Alovisio A, Becerra J. Power cycles integration in concentrated solar power plants with energy storage based on calcium looping. Energy Convers Manage Mar. 2017;149:815–29.
[16] Ortiz C, Valverde J, Chacartegui R, Perez-Maqueda L, Giménez P. The calcium-looping (CaCO3/CaO) process for thermochemical energy storage in concentrating solar power plants. Renew Sustain Energy Rev Oct. 2019;113.
[17] Guelpa E, Tesio U, Verda V. DELIVERABLE D4.2 - Power cycles: schemes, models, analysis. SOlar Calcium-looping integRAtion for Thermo-Chemical Energy Storage, 2019.
[18] Neises T, Turchi C. A comparison of supercritical carbon dioxide power cycle configurations with an emphasis on CSP applications. Energy Procedia 2014;49:1187–96.
[19] Crespi F, Gavagnin G, Sánchez D, Martínez G. Supercritical carbon dioxide cycles for power generation: a review. Appl Energy 2017;195:152–83.
[20] Lazzaretto A, Toffolo A. A method to separate the problem of heat transfer interactions in the synthesis of thermal systems. Energy 2008;33:163–70.
[21] Kemp I. Pinch analysis and process integration. Butterworth-Heinemann; 2007.
[22] Valverde JM, Medina S. Reduction of calcination temperature in the calcium looping process for CO2 capture by using helium: in situ XRD analysis. ACS Sustainable Chem Eng 2016;4:7090–7.
[23] Hanak DP, Manovic V. Calcium looping combustion for high-efficiency low-emission power generation. J Cleaner Prod 2017;161:245–55.
[24] Hanak DP, Manovic V. Calcium looping with supercritical CO2 cycle for decarbonisation of coal-fired power plant. Energy 2016;102:343–53.
[25] Tesio U, Guelpa E, Ortiz C, Chacartegui R, Verda V. Optimized synthesis/design of the carbonator side for direct integration of thermochemical energy storage in size concentrated solar power. Energy Convers Manage 2019;X:100025.
[26] Bell I, Wronski J, Quolin S, Lemort V. Welcome to CoolProp — CoolProp 6.3.0 documentation, [Online]. Available: http://www.coolprop.org/. [Accessed 2019].
[27] Chase M. NIST-JANAF thermochemical tables. Fourth edition. American Institute of Physics; 1998.
[28] SysCAD: Plant Simulation Software, [Online]. Available: https://www.syscad.net/. [Accessed 2019].
[29] Binotti M, Astolfi M, Campanari S, Manzolini G, Silva P. Preliminary assessment of sCO2 power cycles for application to CSP solar tower plants. Energy Procedia 2017;106:1116–22.
[30] Zhu H-H, Wang K, He Y-L. Thermodynamic analysis and comparison for different direct-heated supercritical CO2 Brayton cycles integrated into a solar thermal power tower system. Energy 2017;140:144–57.
[31] Javanshir A, Sarunac N, Razzaghpanah Z. Thermodynamic analysis of simple and regenerative Brayton cycles for the concentrated solar power applications. Energy Convers Manage 2018;163.
[32] Noaman M, Saade G, Morosuk T, Tsatsaronis G. Exergoeconomic analysis applied to supercritical CO2 power systems. Energy 2019;183:756–65.
[33] Penkuhn M, Tsatsaronis G. Exergoeconomic analyses of different sCO2 cycle configurations. The 6th International Symposium – Supercritical CO2 Power Cycles 2018.
[34] Reyes-Belmonte M, Sebastián A, Romero M, González-Aguilar J. Optimization of a recompression supercritical carbon dioxide cycle for an innovative central receiver solar power plant. Energy 2016;112:17–27.
[35] Albrecht K, Carlson M, Ho C. Integration, control, and testing of a high-temperature particle-to-sCO2 heat exchanger. AIP Conf Proc 2019:2126.
[36] Moore J, Cich S, Day S, Allison T, Wade J, Hofer D. Commissioning of a 1 MWe supercritical CO2 test loop. The 6th International Supercritical CO2 Power Cycles Symposium 2018.
[37] Toffolo A. A synthesis/design optimization algorithm for Rankine cycle based energy systems. Energy 2014;66:115–27.
[38] Toffolo A, Lazzaretto A, Morandin M. The HEATSEP method for the synthesis of thermal systems: an application to the S-Graz cycle. Energy 2010;35:976–81.
[39] Mesfun S, Toffolo A. Optimization of process integration in a Kraft pulp and paper mill – evaporation train and CHP system. Appl Energy 2013;107:98–110.
[40] Qiu Y, He Y-L, Du B-C. A comprehensive model for analysis of real-time optical performance of a solar power tower with a multi-tube cavity receiver. Appl Energy 2017;185:589–603.